

3D Mapping of X-Ray Images in Inspections of Aerospace Parts

Daniele Evangelista*, Matteo Terreran*, Alberto Pretto[†], Michele Moro*,
Carlo Ferrari*, and Emanuele Menegatti*

*Department of Information Engineering, University of Padua, Italy
Email: [evangelista, terreran, michele.moro, carlo.ferrari, emg]@dei.unipd.it

[†]IT+Robotics srl, Padua, Italy
Email: alberto.pretto@it-robotics.it

Abstract—In this work we present an industrial system for the inspection of composite parts in the aerospace industry, based on X-ray sensors and robotic manipulators. Such system is designed to identify any type of defects such as, missing gluing, core cell deformation, cracks or foreign objects, which may occur between layers of which these objects are composed. The inspection process involves back-projection of X-ray images onto the 3D CAD model of the inspected part, to directly locate the defects on the part itself. The complete system has been implemented in a real industrial workcell that involves two synchronized robots equipped with a X-ray source-detector system. The two robots move autonomously along a pre-computed trajectory without any human intervention, and the back-projection of the acquired images is efficiently performed at run-time using the proposed algorithm. The experiments demonstrate that the X-ray images back-projection is successful and can effectively replace standard manually guided inspections. This has a high impact on the factory automation cycle since it helps to reduce the effort and time needed for each inspection task. This work is part of a EU funded project called *SPiRiT*.

Index Terms—X-ray imaging, Industrial inspection, 3D metrology, Inspection of composite parts

I. INTRODUCTION

Inspection in industry is a fundamental part of the production chain. For example, in manufacturing industry, products are directly inspected on the production line to detect defects, anomalies and problems that must necessarily be avoided in order to increase the overall quality and productivity of the factory. Although this activity has often been entrusted to human workers in the past [1], with the increasing use of robots in industry, this task has been suddenly demanded to automatic systems, i.e. robot manipulators [2]. Robots are faster than humans, they do not get tired and can also be used in dangerous environments, where human safety cannot be guaranteed (e.g. nuclear and chemical industry).

In this work we present an automatic system to perform X-ray inspection of composite parts in the aerospace industry, as depicted in Figure 1. Such system is part of a wider ongoing project called *SPiRiT*¹, which aims to develop a general soft-

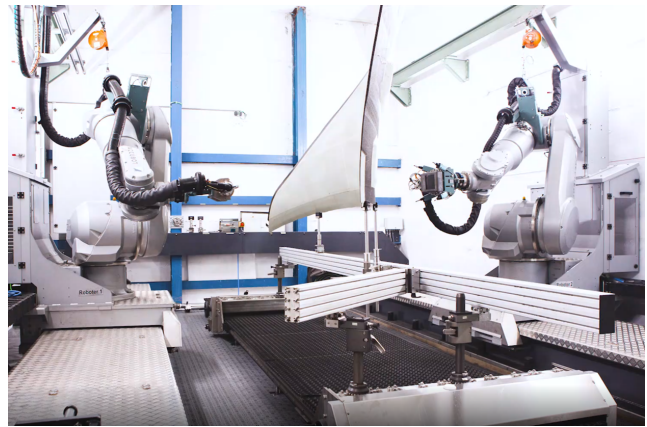


Fig. 1: Example of an X-ray inspection system in the aerospace industry.

ware framework for robotic inspection applicable to different scenarios and different inspection technologies. One particular test case is related to the aerospace industry, with the inspection of carbon fibre reinforced components. These components are usually made of either *Nomex* or aluminium layers and have hexagonally shaped core cells. Most components consist of multiple cores, which are bonded by adhesive foam. X-ray inspection is used to identify defects in the core area, e.g. non-existent bonding, core cell deformation, cracks and foreign objects. The mapping of sensor data is necessary in this type of application because it allows to convert a 2D image sequence into a 3D data map projected on the inspected object. In this way it is possible to overcome multiple problems and difficulties that exist in data analysis based only on 2D images, such as: the management of image borders, the management of overlapping images and the difficulty of identifying the exact position of defects on the part.

The remainder of the paper is structured as follows. Section II reviews the work related to industrial inspection with X-ray sensors in multiple fields. Section III describes our data back-projection algorithm in detail. Section IV shows some qualitative results achieved on a real setup in the aerospace industry, while in Section V conclusions and future directions are provided.

This work is part of the SPiRiT project. The SPiRiT project has received funding from the European Union's Horizon 2020 research and innovation programme under grant agreement No 779431. Part of this work was supported by MIUR (Italian Minister for Education) under the initiative "Departments of Excellence" (Law 232/2016).

¹www.spirit-h2020.eu

II. RELATED WORKS

Industrial inspection is nowadays a common task performed in many sectors using machine vision approaches and different hardware depending on the specific industrial scenario. For example, in the food industry quality inspection is mainly done visually, using cameras to highlight visual features such as color or shape [3] [4]. In automotive and aerospace industry, normal cameras are not suitable for quality inspection of composite parts and carbon fibers, due to the challenging optical properties of such materials. In such cases common solutions are infrared cameras [5], X-ray sensors [6] [7] or specific sensors designed to measure fibre orientation [8]. In wood processing industry, X-ray computed tomography (CT) technology is used for non-invasive assessment of log internal feature, as the geometry and position of knots [9] [10]. In this case, a rotating X-ray source produces cross-sectional images that can be used to generate three-dimensional (3D) reconstructions of the scanned object including information about the outer shape, internal knottiness and identified defects.

Although CT technology outputs very detailed 3D reconstructions, it requires that the part to be inspected is smaller than the CT machine. This could be not possible or unfeasible in particular inspection task, for example when the part is too large or it has a peculiar shape. In this scenario, an alternative approach is X-ray stereo, which uses an X-ray source and a detector for image acquisition [11]. The 3D reconstruction is then obtained with photogrammetric methods combining X-ray images from different point of views.

The inspection process can be further automated using an industrial robotic arm to move a sensor along the part to be inspected while acquiring data. In [12] a specific sensor to measure fibre orientation is mounted on a robot arm. Using such robot arm, the sensor is moved on a predefined path to inspect a carbon fibre part, namely its fibre orientations. The data acquired are then mapped onto the CAD model to obtain a fully 3D representation of the part's fibre angles. In our work, we adopt a similar strategy but using instead X-ray source and detector mounted on individual robotic arms. Moreover, we focus on reconstructing the part's structure given by the hexagonally shaped core cells. X-ray images are directly mapped onto the surface of the CAD model of the part, to obtain a textured CAD model where defects can be easily identified. To our knowledge X-ray mapping on a CAD model has not been applied in a manufacturing context before.

III. MAPPING X-RAY IMAGES ONTO 3D MODELS

X-ray systems in industrial settings strongly differ from medical ones. For example, for medical X-ray systems, the *source* and detector *devices* are usually mounted at the edge of a so-called C-arm rigid structure, it is a C-shaped rigid frame that makes the source and detector positions fixed. For such configuration, the mathematical projection model of the camera can be reduced to the one of standard pinhole cameras, this is done by introducing the so-called *virtual detector plane* [13]. On the other hand, in industrial setups, the X-ray *source* and the *detector* sensor are usually mounted

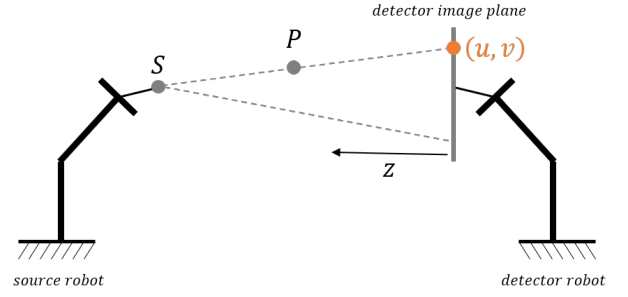


Fig. 2: Source-detector projection model.

on individual robotic arms. These robots are often mutually coupled and their control is synchronized in such a way that the center of the X-ray cone emitted from the *source* is always perpendicular and incident to the center of the *detector* plane.

In the next section the *source-detector* projection model is resumed. This mathematical model has been widely studied and applied in the past [14], and it is one of the key elements of the data back-projection algorithm developed in this work and that will be detailed in section III-B.

A. Source-Detector Projection Model

In Figure 2 the *source-detector* projection model is depicted. In particular, for back-projecting a desired point P onto the image plane of the *detector*, the equations below are used:

$$P' = S + \frac{S_z}{S_z - P_z} (P - S) \quad (1)$$

$$\begin{bmatrix} u \\ v \end{bmatrix} = \begin{bmatrix} f_x & 0 \\ 0 & f_y \end{bmatrix} \begin{bmatrix} P'_x \\ P'_y \end{bmatrix} + \begin{bmatrix} c_x \\ c_y \end{bmatrix}, \quad (2)$$

where P and S represent the position of the desired point and the X-ray source emitter position respectively, all expressed in the *detector* coordinate system using homogeneous representation (i.e. $S = (S_x, S_y, S_z, 1)$). P' is a 3D point expressed in the *detector* coordinate system that represents the intersection between the ray that generates from S , passes through P and intersect the *detector* plane. (c_x, c_y) are the 2D coordinates of the image principal point on the *detector* plane and (f_x, f_y) represent the inverse of the sensor pixel size. In our setup, a *Dexela 1512 NDT* has been used, this sensor has $74.8 \mu m$ pixel size. Finally, (u, v) in Eq.2 are the 2D image coordinates of the back-projected point P on the *detector* image plane.

B. Data Back-Projection

The projection model described above has been used in the data back-projection algorithm described in Algorithm 1. This algorithm computes the set of 2D pixel coordinates for each 3D vertex of the object mesh. In order to increase efficiency and reduce the computational cost for Algorithm 1, the back-projection is done only for those triangles of the mesh that are visible from the given robot and sensor position and that fall within a given *Mask*. In particular, we consider *Mask* as a binary image that is used for excluding some parts of the

Algorithm 1: Data Back-Projection algorithm.

Input: a set of pose-referenced images (I_S, O_S) , the object CAD model Obj , the *Mask* to be applied on the images

Output: the texture coordinates mapping *Map*

$Map \leftarrow \emptyset$;

```
foreach  $(I_i, O_i) \in (I_S, O_S)$  do
   $Pts_i = getVisiblePts(O_i, Obj)$ ;
  foreach  $P_j \in Pts_i$  do
    if  $P_j \notin Map$  then
       $Im_i = applyMask(I_i, Mask)$ ;
       $(u, v)_j = unproj(P_j, Im_i)$ ;
      if  $(u, v)_j \subseteq Im_i$  then
         $Map = Map \cup [(u, v)_j, P_j]$ ;
      else
        continue;
      end
    else
      continue;
    end
  end
end
end
return Map;
```

input image. In our tests, the *Mask* is a variable circle centered in the image centre, it is helpful in this setup because X-ray images suffer from high presence of artifacts at their borders due to non-perpendicularity of the surface normal with the image plane. The visibility check in Algorithm 1 has been implemented using an augmented version of the algorithm for the computation of the intersection of a ray/segment with a triangle introduced in [15].

IV. EXPERIMENTS

A. Experimental Setup

In Figure 3, the real X-ray inspection workcell is depicted. In this setup two *Stäubli 200L* robots have been used. The two robots are mutually synchronized and their control has been properly set in such a way that, while moving, the image plane of the X-ray detector (mounted on the robot on the right) is always perpendicular at the X-ray beam emitted by the source device (mounted on the robot on the left). This is a fundamental constraint that must be ensured in source-detector X-ray inspection systems, because it allows the acquisition of more clear and sharp images. Indeed, the more the X-ray beam is perpendicular to the detector plane, the more we avoid artifacts in the image caused by the overlap of the internal layers of the object.

The part to be inspected, whose CAD model is depicted in Figure 4, is placed in the centre and, as already mentioned, the two robots move synchronously following an off-line pre-computed path. The entire setup is enclosed in a lead chamber that prevents leakage and dispersion of radiation harmful to human operators.

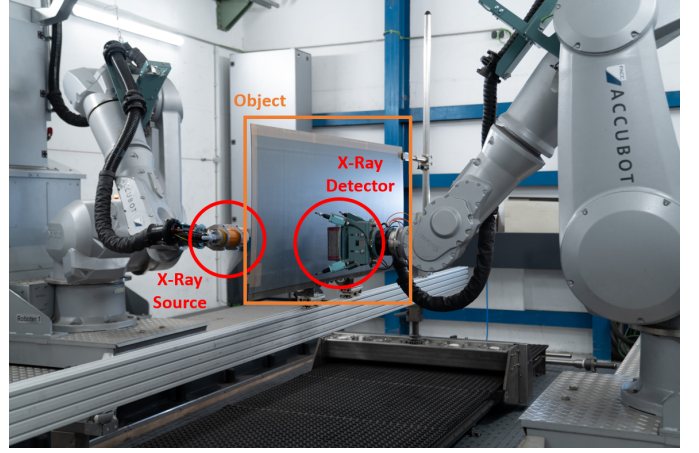


Fig. 3: Experimental setup. The X-ray inspection system is mounted on two *Stäubli 200L* robots at the *FACC GmbH* facility.

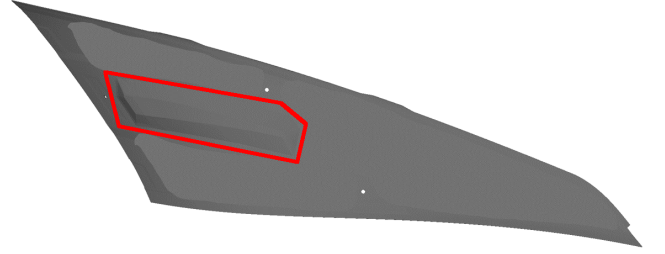


Fig. 4: The rear view of the CAD of the object used for the inspection tests. Proprietary details have been hidden on purpose. In red the part of the model that has been inspected for the tests.

B. Qualitative Results

In Figure 5 some qualitative results of the back-projection algorithm are reported. In this test the robot moved along a predefined path so that to cover a small portion of the whole object. From this initial test it is possible to notice how the back-projection is robust enough to guarantee a qualitatively acceptable result while applying the texture on the 3D model of the object. It must be noticed that no data fusion procedure has been employed yet to when stitching patches of consecutive frames. However, the specific structures in the texture (e.g. honeycomb structure of the *Nomex* core) are consistently maintained. This is a quite reasonable input for further steps of the inspection procedure for detecting possible defects and problems in the object.

V. CONCLUSION

In this work we present an industrial system for the inspection of composite parts in the aerospace industry, based on X-ray sensors and robotic manipulators. The images are directly back-projected on the 3D CAD model of the inspected part and the process is performed at run-time while the robots are moving following a pre-computed trajectory. The results of the back-projection are qualitatively sufficient enough to

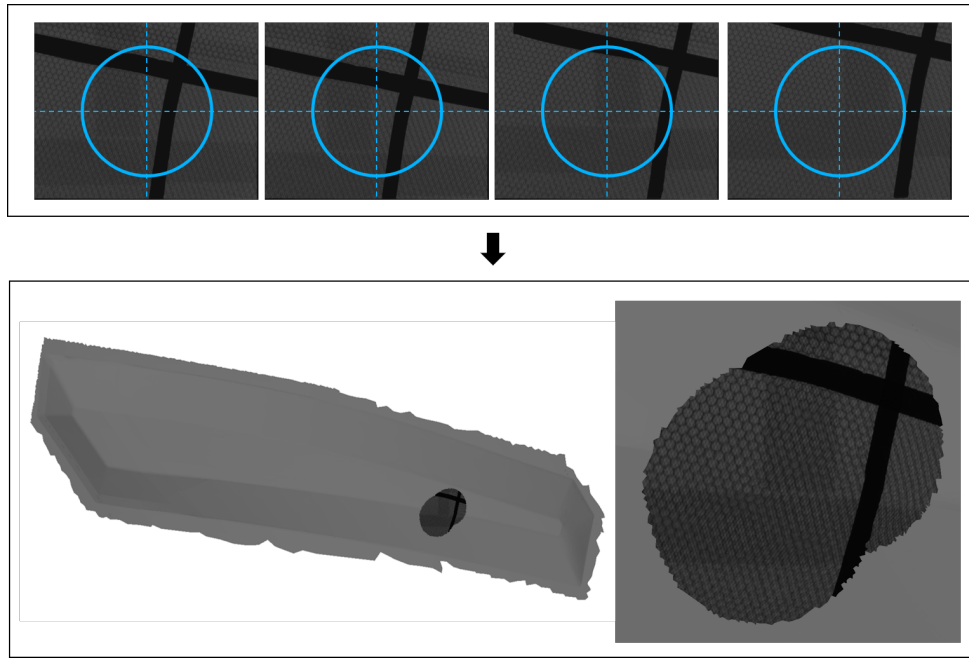


Fig. 5: The top row contains a selection of the X-ray images to be mapped on the object CAD model. The cyan circle in the middle is to show the part of the image that has been involved in the test. Last row contains the back-projection result. Notice that the picture only shows a small sub-part of the entire CAD model, see Figure 4 for further details.

be taken as input for next processing steps where defects can be detected directly on the 3D model of the object. In the near future, we plan to provide a detailed and quantitative analysis of the back-projection procedure, together with an extension of the current approach on different scenarios and inspection technologies such as thermal camera inspections and 3D sensors.

ACKNOWLEDGMENT

The authors would like to acknowledge the industrial partners of the *SPIRIT* project: *Marposs S.p.A.*, *FACC GmbH*, *Centro Ricerche Fiat S.C.p.A.*, *InfraTec GmbH* and *BÖHLER Aerospace GmbH*.

REFERENCES

- [1] E. N. Malamas, E. G. Petrakis, M. Zervakis, L. Petit, and J.-D. Legat, "A survey on industrial vision systems, applications and tools," *Image and Vision Computing*, vol. 21, no. 2, pp. 171 – 188, 2003. [Online]. Available: <http://www.sciencedirect.com/science/article/pii/S026288560200152X>
- [2] P. Kopardekar, A. Mital, and S. Anand, "Manual, hybrid and automated inspection literature and current research," 1993.
- [3] J. C. Noordam, G. W. Otten, T. J. M. Timmermans, and B. H. van Zwol, "High-speed potato grading and quality inspection based on a color vision system," in *Machine Vision Applications in Industrial Inspection VIII*, K. W. T. Jr. and J. C. Stover, Eds., vol. 3966, International Society for Optics and Photonics. SPIE, 2000, pp. 206 – 217. [Online]. Available: <https://doi.org/10.1117/12.380075>
- [4] M. Abdullah, S. Aziz, and A. Mphamed, "Quality inspection of bakery products using a color machine vision system," *Journal of Food Quality - J FOOD QUAL*, vol. 23, pp. 39–50, 03 2000.
- [5] M. Antonello, S. Ghidoni, and E. Menegatti, "Autonomous robotic system for thermographic detection of defects in upper layers of carbon fiber reinforced polymers," in *2015 IEEE International Conference on Automation Science and Engineering (CASE)*. IEEE, 2015, pp. 634–639.
- [6] P. J. Schilling, B. R. Karedla, A. K. Tatiparthi, M. A. Verges, and P. D. Herrington, "X-ray computed microtomography of internal damage in fiber reinforced polymer matrix composites," *Composites Science and Technology*, vol. 65, no. 14, pp. 2071–2078, 2005.
- [7] M. J. Emerson, K. M. Jespersen, A. B. Dahl, K. Conradsen, and L. P. Mikkelsen, "Individual fibre segmentation from 3d x-ray computed tomography for characterising the fibre orientation in unidirectional composite materials," *Composites Part A: Applied Science and Manufacturing*, vol. 97, pp. 83–92, 2017.
- [8] S. Zambal, W. Palfinger, M. Stöger, and C. Eitzinger, "Accurate fibre orientation measurement for carbon fibre surfaces," *Pattern Recognition*, vol. 48, no. 11, pp. 3324–3332, 2015.
- [9] F. Giudiceandrea, E. Ursella, and E. Vicario, "A high speed ct scanner for the sawmill industry," in *Proceedings of the 17th international non destructive testing and evaluation of wood symposium*. University of West Hungary Sopron, Hungary, 2011, pp. 14–16.
- [10] S. M. Stängle, F. Brüchert, A. Heikkilä, T. Usenius, A. Usenius, and U. H. Sauter, "Potentially increased sawmill yield from hardwoods using x-ray computed tomography for knot detection," *Annals of forest science*, vol. 72, no. 1, pp. 57–65, 2015.
- [11] J. A. Noble, R. Gupta, J. Mundy, A. Schmitz, and R. I. Hartley, "High precision x-ray stereo for automated 3d cad-based inspection," *IEEE Transactions on Robotics and automation*, vol. 14, no. 2, pp. 292–302, 1998.
- [12] M. Antonello, M. Munaro, and E. Menegatti, "Efficient measurement of fibre orientation for mapping carbon fibre parts with a robotic system," in *International Conference on Intelligent Autonomous Systems*. Springer, 2016, pp. 757–769.
- [13] N. Navab, M. Mitschke, and O. Schütz, "Camera-augmented mobile c-arm (camc) application: 3d reconstruction using a low-cost mobile c-arm," in *Medical Image Computing and Computer-Assisted Intervention - MICCAI'99*, C. Taylor and A. Colchester, Eds. Berlin, Heidelberg: Springer Berlin Heidelberg, 1999, pp. 688–697.
- [14] D. Mery, D. Hahn, and N. Hitschfeld, "Simulation of defects in aluminium castings using cad models of flaws and real x-ray images," *Insight*, vol. 47, pp. 618–624, 10 2005.
- [15] T. Möller and B. Trumbore, "Fast, minimum storage ray-triangle intersection," *Journal of Graphics Tools*, vol. 2, 08 2005.